Gradient Algorithms for Polygonal Approximation of Convex Contours

Sara Susca [a], Francesco Bullo [a], Sonia Martínez [b]

[a] *Center for Control, Dynamical Systems and Computation, University of California at Santa Barbara, Santa Barbara, CA, 93106-5070, USA. Tel: (+1) 805 893-5169, Fax: (+1) 805 893-8651*

[b] *Mechanical and Aerospace Engineering Department, University of California at San Diego, 9500 Gilman Dr, La Jolla, CA, 92093-0411, USA. Tel: (+1) 858 822-4243, Fax: (+1) 858 534-4387*

Abstract

The subjects of this paper are descent algorithms to optimally approximate a strictly convex contour with a polygon. This classic geometric problem is relevant in interpolation theory and data compression, and has potential applications in robotic sensor networks. We design gradient descent laws for intuitive performance metrics such as the area of the inner, outer, and "outer minus inner" approximating polygons. The algorithms position the polygon vertices based on simple feedback ideas and on limited nearest-neighbor interaction.

Key words: convex body approximation, gradient methods, interpolation, motion coordination.

1 Introduction

In this paper we investigate algorithms to compute an approximating polygon for strictly convex planar contours. We require that the approximating polygon minimizes a certain meaningful error metric. In applications such as monitoring of environmental processes it is important to be able to approximate the contour of the region of interest. Finding efficient or optimal approximating polygons is also relevant in other applications like solving interpolation problems or data compression. Constructing an optimal polygonal approximation of a contour has been a research subject for mathematicians and engineers across the last three centuries. Still interesting problems continue to remain unsolved especially for the general setting of non-convex bodies. Boundary estimation and tracking is also a relevant problem in computer vision [8]. Some references on the boundary estimation problem for robotic sensor networks include [11,3,2,14]. A final motivation for this work is the interest in dynamical systems that solve optimization problems, as described for example in [6]; discrete-time gradient systems and discrete-time balancing algorithms for networks of agents are discussed in [9,1] and in [12].

Email addresses: sara@ece.ucsb.edu (Sara Susca), bullo@engineering.ucsb.edu (Francesco Bullo), soniamd@ucsd.edu (Sonia Martínez).

As pointed out by the authors in [7], in the 19th century it was known how to geometrically characterize the polygon enclosed in a convex body that minimizes the area difference between itself and the enclosing convex body. On the other hand, the geometric characterization of a polygon, enclosing a given strictly convex body, that again minimizes the difference of the areas is more complex and less intuitive. To the best of our knowledge, the earliest reference on this matter appeared only in 1949 by Trost, see [13]. In the 20th century it was also proved that for a convex planar body the approximation error, for various useful metrics, goes to zero as $1/N^2$, where N is the number of vertices of the interpolating polygon. For a detailed list of references we refer to the survey [5].

Given N points (ordered in a counter-clockwise fashion) on a strictly convex contour, it is natural to define an enclosed (i.e., inscribed) polygon and an enclosing (i.e., circumscribed) polygon to the contour. Here the faces of the enclosing polygon are subsets of the tangent lines to the strictly convex contour. We adopt three geometrically-motivated error metrics that the approximating polygon can minimize. They are described as follows. The first two metrics we consider are the difference between the area enclosed in the contour and the following areas: the inner polygon area and the outer polygon area. The third metric is the difference between the area of the outer polygon and the area of the inner

polygon. We derive the expressions, two of which are novel contributions of this paper, of the error metrics as functions of the vertex positions of the approximating polygon. We propose three gradient descent vector fields for N points to dynamically construct the optimal approximating polygon. The vector fields rely only on local information about the contour and about the immediate clockwise and counter-clockwise neighboring vertices. This property allows the vector fields to be implemented by a network of robots. The robots, placed around the boundary of a convex set, have to be able to sense the tangent of the set, to communicate with each other, and to move. We analyze the dynamical system behavior of these vector fields and present simulation results. We also present discrete-time versions that allows the nodes to reach locally optimal configurations for two of the metrics introduced.

The paper is organized as follows. In Section 2 we define some notation and the three performance metrics. In Sections 3 and 4 we present the continuous time gradient descent algorithms and their respective discrete-time algorithms to compute the best inner and outer approximating polygon, while in Section 5 we present an algorithm to construct the polygon minimizing the "outer minus inner" area. In Section 6 we present some simulation results.

2 Problem setup

We review some basic notions on the differential geometry of curves from [4]. Let $Q \subseteq \mathbb{R}^2$ be a compact, strictly convex body with a twice differentiable boundary ∂Q. Let $\gamma\colon [0, \text{length}(\partial Q)] \to \partial Q$ be the counter-clockwise arclength parametrization of ∂Q. For $s \in [0, \text{length}(\partial Q)]$, define the tangent vector $\mathbf{t}(s) = \gamma'(s)$ and the unit inward normal vector $\mathbf{n}(s)$ at $\gamma(s) \in \partial Q$. We then define the curvature $\kappa\colon [0, \text{length}(\partial Q)] \to \mathbb{R}_{>0}$ by requiring that it satisfies

$$\frac{d\mathbf{t}(s)}{ds} = \kappa(s)\mathbf{n}(s), \quad \frac{d\mathbf{n}(s)}{ds} = -\kappa(s)\mathbf{t}(s). \qquad (1)$$

With these conventions, the curvature is strictly positive since Q is strictly convex. For $p \in \partial Q$, define the half-plane $\mathcal{H}(p) = \{z \in \mathbb{R}^2 \mid (p - z) \cdot \mathbf{n}(p) \geq 0\}$. Given two points A and B, we let $\overline{AB}$ denote the segment between them. In what follows, whenever we consider N points $p_1, \ldots, p_N$ on ∂Q, we shall (i) assume that they are ordered counter-clockwise, (ii) assume that $N \geq 3$, and (iii) use the identification $0 \equiv N$ and $N + 1 \equiv 1$. With a slight abuse of notation, we sometimes refer to tangent and normal vectors at $p \in \partial Q$ as $\mathbf{t}(p)$ and $\mathbf{n}(p)$, and at p_i as $\mathbf{t}_i$ and $\mathbf{n}_i$.

Definition 2.1 (Inner and outer polygons) *Let $p_1, \ldots, p_N$ be the positions of N points on ∂Q and let $\mathcal{P}(\mathbb{R}^2)$ denote the parts of $\mathbb{R}^2$. Let us define $P_I\colon (\partial Q)^N \to \mathcal{P}(\mathbb{R}^2)$ by $P_I(p_1, \ldots, p_N) = \text{co}(p_1, \ldots, p_N)$, the* inner polygon *generated by the vertices $\{p_1, \ldots, p_N\}$. With a slight abuse of notation, let us define the* possibly unbounded outer polygon *$P_O\colon (\partial Q)^N \to \mathcal{P}(\mathbb{R}^2)$ by $P_O(p_1, \ldots, p_N) = \mathcal{H}(p_1) \cap \cdots \cap \mathcal{H}(p_N)$.*

Definition 2.2 (Tangent lines and tangent connections) *Define the rays $\ell^+\colon \partial Q \to \mathcal{P}(\mathbb{R}^2)$ and $\ell^-\colon \partial Q \to \mathcal{P}(\mathbb{R}^2)$ by $\ell^+(p) = \{p + \lambda\mathbf{t}(p) \mid \lambda \geq 0\}$ and $\ell^-(p) = \{p + \lambda\mathbf{t}(p) \mid \lambda \leq 0\}$, respectively. Also, let $\ell(p) = \ell^+(p) \cup \ell^-(p)$. A pair (p, q) of points in ∂Q is* counter-clockwise tangent-connected *(abbreviated cc-tangent-connected) if $\ell^+(p) \cap \ell^-(q) \neq \emptyset$.*

Lemma 2.3 (Bounded outer polygon) *The polygon $P_O(p_1 \ldots, p_N)$ is bounded if and only if all pairs (p_i, p_{i+1}), $i \in \{1, \ldots, N\}$, are cc-tangent-connected.*

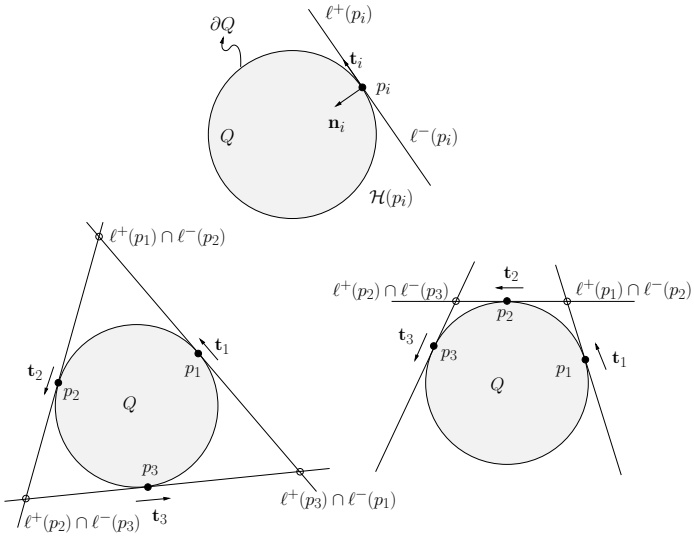

Fig. 1. Basic notation. Three points defining a bounded outer polygon. Three points defining an unbounded outer polygon.

This result is illustrated in Figure 1. Next, we quantify the approximation error via three different metrics.

Definition 2.4 (Error metrics) *Define the* inner set approximation error *E_I, the* outer set approximating error *E_O, and the* symmetric difference error *E_S as functions from $(\partial Q)^N$ to $\mathbb{R}_{\geq 0} \cup \{+\infty\}$ defined by, respectively,*

$$E_I(p_1, \ldots, p_N) = \text{Area}(Q \setminus P_I(p_1, \ldots, p_N)),$$
$$E_O(p_1, \ldots, p_N) = \text{Area}(P_O(p_1, \ldots, p_N) \setminus Q),$$
$$E_S(p_1, \ldots, p_N) = \text{Area}(P_O(p_1, \ldots, p_N) \setminus P_I(p_1, \ldots, p_N)).$$

Remark 2.5 (Implementation by group of robots) In what follows we present descent algorithms for the minimization of these error metrics. The algorithms can be implemented by group of robots where we regard p_i as a robot that can sense a portion of ∂Q, communicate with some robots and move to improve the approximation of ∂Q. For all the algorithms that follow we establish how much sensing and communication are required. •

3 Inner-polygon approximation algorithms

The algorithms of this section are based on the interpolation error E_I. Observe that $E_I(p_1,\dots,p_N) = \text{Area}(Q) - \text{Area}(P_I(p_1,\dots,p_N))$. Recalling that the points $p_1,\dots,p_N$ are ordered counter-clockwise, if (x_i, y_i) are coordinates of p_i, then one can show

$$\text{Area}(\mathcal{P}_I(p_1,\dots,p_N)) = \frac{1}{2}\sum_{i=1}^{N}(x_i y_{i+1} - x_{i+1} y_i)\,.$$

We now define a dynamical system by projecting the ith component of the gradient of E_I on the tangent $\mathbf{t}_i$:

$$\begin{aligned}\dot{p}_i &= \left(\mathbf{t}_i \cdot \frac{\partial\,\text{Area}(P_I(p_1,\dots,p_N))}{\partial p_i}\right)\mathbf{t}_i \qquad (2)\\ &= \left(\frac{1}{2}\,\mathbf{t}_i \cdot \begin{pmatrix} y_{i+1} - y_{i-1} \\ x_{i-1} - x_{i+1}\end{pmatrix}\right)\mathbf{t}_i\,, \quad i \in \{1,\dots,N\}\,.\end{aligned}$$

Lemma 3.1 (Gradient flow for E_I) *If $t \mapsto \eta(t) = (p_1(t),\dots,p_N(t))$ denotes a trajectory of the dynamical system (2), then $E_I \circ \eta$ is monotonic non-increasing and η converges asymptotically to the set of critical configurations of E_I. A configuration $p_1,\dots,p_N$ is critical for E_I if and only if, for all $i \in \{1,\dots,N\}$,*

$$\mathbf{t}_i \perp \begin{pmatrix} y_{i+1} - y_{i-1} \\ x_{i-1} - x_{i+1}\end{pmatrix}, \qquad (3)$$

that is, $\mathbf{n}_i \perp (p_{i+1} - p_{i-1})$. Furthermore, if the boundary ∂Q is analytic, then η converges asymptotically to a critical configuration.

PROOF. By design the dynamical system (2) is a gradient system. As a consequence, E_I is monotonic non-increasing:

$$\begin{aligned}&\frac{d}{dt}E_I(p_1(t),\dots,p_N(t))\\ &\quad= -\frac{d}{dt}\,\text{Area}(\mathcal{P}_I(p_1(t),\dots,p_N(t)))\\ &\quad= -\sum_{i=1}^{N}\left(\mathbf{t}_i \cdot \frac{\partial\,\text{Area}(P_I(p_1,\dots,p_N))}{\partial p_i}\right)^2 \le 0,\end{aligned}$$

and the p_i's asymptotically converge to the set of critical configurations of E_I. If the boundary ∂Q is analytic, then E_I is analytic (because it is a composition of analytic functions) and, by [10], we can conclude that every trajectory has finite length and tends to a single point belonging to the set of critical configurations. □

Not every critical point of E_I is an extremum of E_I: Figure 2 illustrates a saddle point of E_I.

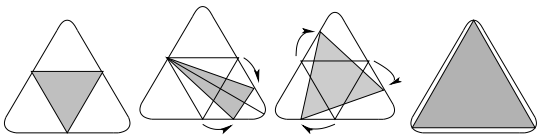

Fig. 2. From left to right: saddle point configuration, nearby configuration that increases the error E_I, bear by configuration that decreases the error E_I, configuration corresponding to a minimum error configuration.

Remark 3.2 (Historical notes) According to [7], the characterization (3) of the critical configurations was already obtained in the 19th century and the critical point configurations have the property that the point density is higher in regions of higher mean curvature. It is believed [5] that as the number of nodes increases, the type of configurations that satisfy (3) correspond only to global error minima. •

Remark 3.3 (Implementation by group of robots) In the dynamical system (2), the velocity $\dot{p}_i$ depends only on p_{i-1}, p_{i+1}, and $\mathbf{t}_i$. Therefore, to implement this velocity control, every robot has to receive information about the positions of its immediate clockwise and counter-clockwise neighbors and sense the gradient of the contour at its position. Clearly, the communication graph is a ring graph. •

3.1 Discrete-time inner-polygon approximation algorithms

Here we present two discrete-time versions of the vector field in equation (2). Given a strictly convex set Q, define $q_{\max}\colon (\partial Q)^2 \to \partial Q$ as follows: $q_{\max}(q_1, q_2)$ is the point of the counter-clockwise arc from q_1 to q_2 whose tangent to ∂Q is parallel to the segment $\overline{q_1 q_2}$. Since Q is strictly convex, the tangent point is unique and $q_{\max}$ is well defined.

Algorithm 1. At each discrete time instant $k \in \mathbb{N}$ and for each node $i \in \{1,\dots,N\}$ define:

$$p_i(k{+}1) = \begin{cases} q_{\max}(p_{i-1}(k), p_{i+1}(k)), & \text{if } i \equiv k \mod N,\\ p_i(k), & \text{if } i \not\equiv k \mod N\,.\end{cases} \qquad (4)$$

Theorem 3.4 (Convergence of Algorithm 1) *If $k \mapsto \eta(k) = (p_1(k),\dots,p_N(k))$ denotes a trajectory of the dynamical system (4), then $E_I \circ \eta$ is monotonic non-increasing and η converges asymptotically to the set of critical configurations of E_I.*

PROOF. First, note that $q_{\max}(q_1, q_2)$ is the unique global maximum of the strictly concave function $q \mapsto \text{Area}(P_I(q_1, q, q_2))$. Next, let $i = k \mod N$ and let $A_k = \text{Area}(P_I(p_1(k),\dots,p_N(k))$. We have that $A_k = T_k + \bar{A}_k$, where $T_k = \text{Area}(P_I(p_{i-1}(k), p_i(k), p_{i+1}(k))$ and

$\bar{A}_k = \text{Area}(P_I(p_{i-1}(k), p_{i+1}(k), \ldots, p_{i-2}(k))$. Because of the global maximum property of $q_{\max}(q_1, q_2)$, we have that $T_k = \text{Area}(P_I(p_{i-1}(k), p_i(k), p_{i+1}(k)) \leq \bar{T}_{k+1}$, where $\bar{T}_{k+1} = \text{Area}(P_I(p_{i-1}(k), p_i(k+1), p_{i+1}(k))$. Therefore, $A_k = T_k + \bar{A}_k \leq \bar{T}_{k+1} + \bar{A}_k = A_{k+1}$, i.e., each point moves in order to not decrease the area of the inner polygon. Furthermore, unless $p_i(k) = q_{\max}(p_{i-1}(k), p_{i+1}(k))$, we have $T_k < \bar{T}_{k+1}$ and $A_k < A_{k+1}$ because of the strict global maximum property of $q_{\max}$. Therefore, by the LaSalle Invariance Principle, the trajectories of Algorithm 1 converge to the set of configurations such $\{(p_1(k), \ldots, p_N(k)) \in (\partial Q)^N |\ p_i = q_{\max}(p_{i-1}, p_{i+1})\ i \in \{1, \ldots, N\}\}$. By equation (3) this set is the set of critical configurations of E_I. □

At this point, a natural question of interest is whether one may modify Algorithm 1 to allow multiple nodes to move simultaneously while preserving its convergence properties. In what follows we partially answer this question by introducing an "admissible quintuplet" of points. Precisely speaking, the quintuplet $(p_{-2}, p_{-1}, p_0, p_1, p_2)$ is *admissible* if the following three inequalities hold:

$$\begin{aligned}
&\text{Area}(P_I(q_{\max}(p_{-2}, p_0), p_0, q_{\max}(p_0, p_2))) \\
&\quad \leq \text{Area}(P_I(q_{\max}(p_{-2}, p_0), q_{\max}(p_{-1}, p_1), q_{\max}(p_0, p_2))), \\
&\text{Area}(P_I(p_{-1}, p_0, q_{\max}(p_0, p_2))) \\
&\quad \leq \text{Area}(P_I(p_{-1}, q_{\max}(p_{-1}, p_1), q_{\max}(p_0, p_2))), \\
&\text{Area}(P_I(q_{\max}(p_{-2}, p_0), p_0, p_1)) \\
&\quad \leq \text{Area}(P_I(q_{\max}(p_{-2}, p_0), q_{\max}(p_{-1}, p_1), p_1)).
\end{aligned}$$

Algorithm 2. At each discrete time instant $k \in \mathbb{N}$ and for each node $i \in \{1, \ldots, N\}$ define:

$$p_i(k+1) = q_{\max}(p_{i-1}(k), p_{i+1}(k)), \tag{5}$$

if $(p_{i-2}(k), p_{i-1}(k), p_i(k), p_{i+1}(k), p_{i+2}(k))$ is admissible, and $p_i(k+1) = p_i(k)$ otherwise.

Theorem 3.5 (Convergence of Algorithm 2) *E_I is monotonic non-increasing along all trajectories of* (5).

PROOF. The proof consists of two parts. As first fact (i), we prove inductively that the area of any polygon of N vertices increases by leaving any two consecutive nodes fixed and by moving the other $N-2$ vertices according to (5). As second fact (ii), building on the previous result, we show that the area of any polygon of N vertices increases by moving the all the N vertices according to (5).

Let us prove first (i) by induction on the number of vertices of a polygon. Let us consider $N = 3$. Clearly, if two of the three vertices are fixed and the other one moves according to (5), the area of the triangle formed by the three nodes increases, just as seen for Algorithm 1. Assume now that, given a polygon $P_I(p_1, \ldots, p_{N-1})$ with $N-1$ vertices, its area can be increased by leaving any two consecutive nodes fixed and moving the other $N-1-2$ vertices according to (5). Let us now prove that the same property holds for the polygon $P_I(p_1, \ldots, p_N)$ with N vertices. Clearly, we have that:

$$\begin{aligned}
\text{Area}(P_I(p_1, \ldots, p_N)) = &\text{Area}(P_I(p_1, \ldots, p_{N-1})) \\
&+ \text{Area}(P_I(p_{N-1}, p_N, p_1)),
\end{aligned}$$

where for simplicity of notation we dropped the time index k. By assumption, the area of a polygon with $N-1$ vertices increases if any two consecutive points are fixed and the rest moves according to (5). Therefore, we have

$$\begin{aligned}
&\text{Area}(P_I(p_1, p_2 \ldots, p_{N-2}, p_{N-1})) \\
&\qquad \leq \text{Area}(P_I(p_1, p_2^+ \ldots, p_{N-2}^+, p_{N-1})),
\end{aligned}$$

where for simplicity of notation the superscript + indicates that the node has updated its position according to (5). This implies:

$$\begin{aligned}
&\text{Area}(P_I(p_1, \ldots, p_N)) \\
&\leq \text{Area}(P_I(p_1, p_2^+ \ldots, p_{N-2}^+, p_{N-1})) + \text{Area}(P_I(p_{N-1}, p_N, p_1)) \\
&= \text{Area}(P_I(p_2^+ \ldots, p_{N-2}^+, p_{N-1}, p_N)) + \text{Area}(P_I(p_N, p_1, p_2^+)) \\
&\leq \text{Area}(P_I(p_2^+ \ldots, p_{N-2}^+, p_{N-1}, p_N)) + \text{Area}(P_I(p_N, p_1^+, p_2^+)) \\
&= \text{Area}(P_I(p_1^+, p_2^+, \ldots, p_{N-2}^+, p_{N-1}, p_N)).
\end{aligned}$$

The second inequality holds because along the trajectories of (5) we have that $\text{Area}(P_I(p_N, p_1, p_2^+)) \leq \text{Area}(P_I(p_N, p_1^+, p_2^+))$. This concludes the proof of (i). To prove (ii), note that

$$\begin{aligned}
&\text{Area}(P_I(p_1^+, p_2^+, \ldots, p_{N-2}^+, p_{N-1}, p_N)) \\
&= \text{Area}(P_I(p_1^+, \ldots, p_{N-2}^+, p_{N-1})) + \text{Area}(P_I(p_{N-1}, p_N, p_1^+)) \\
&\leq \text{Area}(P_I(p_1^+, \ldots, p_{N-2}^+, p_{N-1})) + \text{Area}(P_I(p_{N-1}, p_N^+, p_1^+)) \\
&= \text{Area}(P_I(p_N^+, p_1^+, \ldots, p_{N-2}^+)) + \text{Area}(P_I(p_{N-2}^+, p_{N-1}, p_N^+)) \\
&\leq \text{Area}(P_I(p_N^+, p_1^+, \ldots, p_{N-2}^+)) + \text{Area}(P_I(p_{N-2}^+, p_{N-1}^+, p_N^+)) \\
&= \text{Area}(P_I(p_1^+, \ldots, p_N^+)). \qquad \square
\end{aligned}$$

Remark 3.6 As established in Theorem 3.4 for Algorithm 1, every time a node moves according to Algorithm 2 the area increases strictly. On the other hand, stationary configurations of (5) are not necessarily critical points of E_I, i.e., at an equilibrium configuration for (5) there could exist a node for which condition (3) is not satisfied. A set of nodes could be "unlocked" by running some iterations of Algorithm 1. •

Remark 3.7 (Implementation by group of robots) To implement Algorithm 1, each robot p_i needs to have knowledge about its own label number $i \in \{1, \ldots, N\}$

and about the position of its one-hop neighbors. Algorithm 2, does not require a labeling of robots, but requires each robot to have knowledge about part of the contour and knowledge about the position of its two-hop neighbors. •

4 Outer-polygon approximation algorithms

The algorithms of this section are based on the interpolation error E_O. We begin with a geometric characterization of the partial derivative of E_O and of the critical configurations for E_O. Assuming the pairs (p_{i-1}, p_i) and (p_i, p_{i+1}) are cc-tangent-connected, as depicted in Figure 4, we define the points $A_i = \ell^-(p_i) \cap \ell^+(p_{i-1})$ and $B_i = \ell^-(p_{i+1}) \cap \ell^+(p_i)$ and the nonnegative segment lengths $d_i^- = \text{length}(\overline{p_i A_i})$ and $d_i^+ = \text{length}(\overline{p_i B_i})$. By

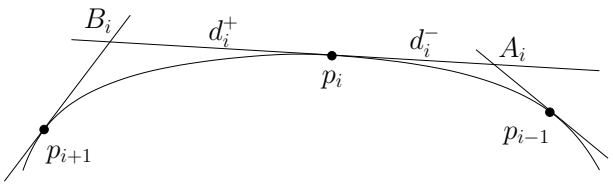

Fig. 3. The points A_i, B_i and the lengths d_i^-, d_i^+

continuity we define $d_i^+(p,p) = d_i^-(p,p) = 0$, for all p. Instead, if (p_i, p_{i+1}) is not cc-tangent-connected, then we set $d_i^+ = +\infty$; and if (p_{i-1}, p_i) is not cc-tangent-connected, then $d_i^- = +\infty$. For p_i distinct from p_{i-1} and p_{i+1}, some trigonometric arguments show that

$$d_i^-(p_i, p_{i-1}) = \begin{cases} +\infty\,, & \text{if } \mathbf{t}_i \cdot \mathbf{n}_{i-1} \le 0\,, \\ \dfrac{(p_i - p_{i-1}) \cdot \mathbf{n}_{i-1}}{\mathbf{t}_i \cdot \mathbf{n}_{i-1}}\,, & \text{otherwise}\,, \end{cases}$$

$$d_i^+(p_i, p_{i+1}) = \begin{cases} +\infty\,, & \text{if } \mathbf{t}_i \cdot \mathbf{n}_{i+1} \ge 0\,, \\ \dfrac{(p_{i+1} - p_i) \cdot \mathbf{n}_{i+1}}{\mathbf{t}_i \cdot \mathbf{n}_{i+1}}\,, & \text{otherwise}\,. \end{cases}$$

Proposition 4.1 (Partial derivative of E_O) *If all pairs (p_i, p_{i+1}) are cc-tangent-connected, then*

$$\frac{\partial E_O(p_1, \ldots, \gamma(s_i), \ldots, p_N)}{\partial s_i} = \frac{1}{2}\big((d_i^-)^2 - (d_i^+)^2\big)\kappa(s_i).$$

PROOF. Pick $\delta s_i > 0$ sufficiently small so that $\gamma(s_i + \delta s_i)$ is a point on the arc from $p_i = \gamma(s_i)$ to p_{i+1}, as shown in Figure 4. Let $D = \ell^+(s_i) \cap \ell^-(s_i + \delta s_i)$. Define the triangle $\mathcal{T}_A$ with vertices D, $A(s_i)$, and $A(s_i + \delta s_i)$, and the triangle $\mathcal{T}_B$ with vertices D, $B(s_i)$, and $B(s_i + \delta s_i)$. By construction:

$$\begin{aligned} E_O(p_1, \ldots, \gamma(s_i + \delta s_i), \ldots p_N) - E_O(p_1, \ldots, \gamma(s_i), \ldots, p_N) \\ = \text{Area}(\mathcal{T}_A) - \text{Area}(\mathcal{T}_B). \end{aligned}$$

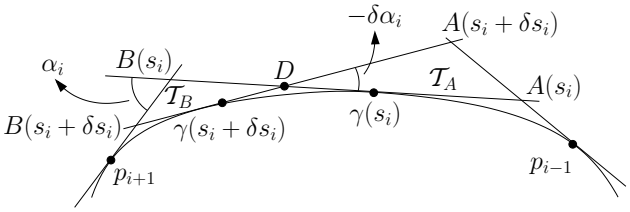

Fig. 4. Notation used in the proof of Proposition 4.1.

Therefore, to compute the variation of E_O, we compute the areas of the two triangles. We begin with some notation. Let $\alpha(s_i)$ be the counter-clockwise angle from $\mathbf{t}_i = \mathbf{t}(s_i)$ to $\mathbf{t}_{i+1}$; if the angle $\angle\mathbf{t}(s_i)$ denotes the orientation of $\mathbf{t}(s_i)$ (measured counter-clockwise from some reference orientation), then $\alpha(s_i) = \angle\mathbf{t}_{i+1} - \angle\mathbf{t}(s_i)$. Note that equation (1) implies $\partial\angle\mathbf{t}(s_i)/\partial s_i = \kappa(s_i)$ so that $\partial\alpha(s_i)/\partial s_i = -\kappa(s_i)$. Next, let $\delta\alpha_i = \alpha(s_i + \delta s_i) - \alpha(s_i)$. Therefore, $\delta\alpha_i = -\kappa(s_i)\delta s_i + o(\delta s_i^2)$. Note that, because Q is strictly convex and p_i, p_{i+1} are ordered counter-clockwise, we have $\alpha(s_i) > 0$ and $\delta\alpha_i < 0$. We are now ready to use some trigonometry to compute the area of $\mathcal{T}_A$. Because $\|\gamma(s_i + \delta s_i) - \gamma(s_i)\| = \delta s_i + o(\delta s_i^2)$, we know that $\|D - A(s_i)\| = d_i^- + \frac{1}{2}\delta s_i + o(\delta s_i^2)$. Now, let h be the height of the triangle $\mathcal{T}_A$ with respect to the base segment from D to $A(s_i)$. Clearly, we have $h = \|A(s_i) - A(s_i + \delta s_i)\| \sin(\alpha(s_{i-1}))$ and

$$\frac{\|A(s_i) - A(s_i + \delta s_i)\|}{\sin(-\delta\alpha(s_i))} = \frac{\|D - A(s_i)\|}{\sin(\pi - (\alpha(s_{i-1}) - \delta\alpha_i))},$$

and, therefore,

$$h = \|D - A(s_i)\| \frac{\sin(-\delta\alpha_i)}{\sin(\alpha(s_{i-1}) - \delta\alpha_i)} \sin(\alpha(s_{i-1})).$$

We have then:

$$\text{Area}(\mathcal{T}_A) = \frac{1}{2}\|D - A(s_i)\|^2 \frac{\sin(\alpha(s_{i-1}))}{\sin(\alpha(s_{i-1}) - \delta\alpha_i)} \sin(-\delta\alpha_i).$$

For small δs_i and $\delta\alpha_i$, we have that $\frac{\sin(\alpha(s_{i-1}))}{\sin(\alpha(s_{i-1}) - \delta\alpha_i)} = 1 + o(\delta\alpha_i)$, and $\sin(-\delta\alpha_i) = -\delta\alpha_i + o(\delta\alpha_i^2)$. Therefore:

$$\text{Area}(\mathcal{T}_A) = \frac{1}{2}(d_i^-)^2(-\delta\alpha_i) + o(\delta\alpha_i^2).$$

Analogously, it can be proved that $\text{Area}(\mathcal{T}_B) = \frac{1}{2}(d_i^+)^2(-\delta\alpha_i) + o(\delta\alpha_i^2)$. Finally, for $p_i = \gamma(s_i)$,

$$\begin{aligned} \frac{\partial E_O(p_1, \ldots, p_N)}{\partial s_i} &= \lim_{\delta s_i \to 0^+} \frac{\text{Area}(\mathcal{T}_A) - \text{Area}(\mathcal{T}_B)}{\delta s_i} \\ &= \lim_{\delta s_i \to 0^+} \frac{-1}{2}\big((d_i^-)^2 - (d_i^+)^2\big)\frac{\delta\alpha_i}{\delta s_i} \\ &= \frac{1}{2}\big((d_i^-)^2 - (d_i^+)^2\big)\kappa(s_i). \qquad \square \end{aligned}$$

We are now ready to propose a gradient-like dynamical system for E_O. First, recall from Lemma 2.3 that E_O is well-defined only for configurations that are pairwise cc-tangent-connected. When a pair (p_i, p_{i+1}) is not cc-tangent-connected, the distance functions d_i^+ and d_{i+1}^- are unbounded and the partial derivative of E_0 is ill-defined (note indeed the assumption of Proposition 4.1). To define a globally well-posed dynamical system, we introduce a saturation function. Pick a positive number v and define $\mathrm{sat}_v \colon \mathbb{R} \cup \{+\infty, -\infty\} \to [-v, v]$ by:

$$\mathrm{sat}_v(x) = \begin{cases} x, & x \in [-v, v], \\ +v, & x \in]v, +\infty[\cup \{+\infty\}, \\ -v, & x \in]-\infty, -v[\cup \{-\infty\}. \end{cases}$$

Next, we define the dynamical system

$$\dot{p}_i = \mathrm{sat}_v((d_i^+)^2 - (d_i^-)^2)\, \mathbf{t}_i\,, \qquad i \in \{1, \ldots, N\}. \quad (6)$$

where we adopt the usual conventions regarding operations in $\mathbb{R} \cup \{+\infty, -\infty\}$. It can be checked that the right hand side of (6) is Lipschitz. We are ready for the main result of this section; note that the characterization of the critical points of E_O was originally given in [13].

Theorem 4.2 (Gradient flow for E_O) *If $t \mapsto \eta(t) = (p_1(t), \ldots, p_N(t))$ denotes a trajectory of the dynamical system (6), then (i) $E_O \circ \eta$ is bounded in finite time and monotonic non-increasing afterwards, and (ii) η converges asymptotically to the set of critical configurations of E_O. A configuration $p_1, \ldots, p_N$ is critical for E_O if and only if, for all $i \in \{1, \ldots, N\}$,*

$$d_i^+(p_i, p_{i+1}) = d_i^-(p_i, p_{i-1}).$$

Furthermore, if the boundary ∂Q is analytic, then η converges asymptotically to a critical configuration.

PROOF. Suppose that there exists $i \in \{1, \ldots, N\}$ such that (p_i, p_{i+1}) is not cc-tangent-connected (i.e., $d_i^- < +\infty$ and $d_i^+ = +\infty$). Since $d_i^+ = +\infty$ also $d_{i+1}^- = +\infty$ and E_O is unbounded. Since Q is strictly convex, we have $d_j^- < +\infty$ (resp. $d_j^+ < +\infty$), for all $j \notin \{i, i+1\}$. Because of equation (6), p_i will move counter-clockwise with speed $v > 0$, while p_{i+1} will move clockwise with the same speed. Therefore, in finite time the two rays ℓ_i^+ and ℓ_{i+1}^- intersect, (p_i, p_{i+1}) become cc-tangent-connected and E_O becomes bounded. Now, we prove that, if all pairs (p_i, p_{i+1}) are cc-tangent-connected, then $E_O \circ \eta$ decreases. This implies that, once a cc-tangent-connected configuration is reached, the subsequent configurations remain cc-tangent-connected. Clearly, equation (6) is equivalent to

$$\dot{s}_i = \mathrm{sat}_v((d_i^+)^2 - (d_i^-)^2),$$

and, therefore:

$$\begin{aligned} &\frac{d}{dt} E_O(p_1, \ldots, \gamma(s_i(t)), \ldots, p_N) \\ &\quad = \sum_{i=1}^{N} \frac{\partial E_O(p_1, \ldots, p_N)}{\partial s_i} \dot{s}_i \\ &\quad = \frac{1}{2} \sum_{i=1}^{N} \kappa(s_i)\, ((d_i^-)^2 - (d_i^+)^2)\, \mathrm{sat}_v((d_i^+)^2 - (d_i^-)^2). \end{aligned}$$

Because the curvature κ is strictly positive on the entire boundary, the cost function E_O decreases monotonically along the trajectories of equation (6). Invoking the LaSalle Invariance Principle, we know that the p_i's will asymptotically converge to the set of critical configurations for E_O.

Let $\mathbf{s}(t) = [s_1(t), \ldots, s_N(t)] \in [0, \mathrm{length}(\partial Q)]^N$, and note that if ∂Q is analytic then E_O is analytic on the set of configurations $p_1, \ldots, p_N$ that are pairwise cc-tangent-connected. Next, we recall a result from [9]; see also [1]. If there exists $\delta > 0$ and τ such that, for all $t > \tau$,

$$\frac{dE_O}{dt} = \frac{\partial E_O}{\partial \mathbf{s}} \cdot \dot{\mathbf{s}}(t) \leq -\delta \|\nabla E_O(\mathbf{s}(t))\| \|\dot{\mathbf{s}}(t)\|,$$

then $\mathbf{s}(t)$ converges to a unique critical configuration $\mathbf{s}^*$. We use this result as follows. Note that as $t \to +\infty$, $\mathbf{s}(t)$ approaches the set of critical configurations. We can then conclude that there exists a time τ after which sat_v is not active any longer and, hence, $\dot{s}_i(t) = -\lambda_i(t) \frac{\partial E_O}{\partial s_i}$, where $\lambda_i(t) = \frac{2}{\kappa(s_i)}$. Therefore, with the abbreviation $\frac{\partial E_O}{\partial \mathbf{s}} = \nabla E_O$, we have

$$\begin{aligned} \nabla E_O(\mathbf{s}(t)) \cdot \dot{\mathbf{s}}(t) &= -\nabla E_O(\mathbf{s}(t))^T \Lambda(t) \nabla E_O(\mathbf{s}(t)) \\ &\leq -\lambda_{\min}(t) \|\nabla E_O(\mathbf{s}(t))\|^2\,, \end{aligned}$$

where $\Lambda(t) \in \mathbb{R}^{N \times N}$ is a diagonal matrix with entries $[\Lambda(t)]_{ii} = \lambda_i(t) > 0$, and $\lambda_{\min}(t) = \min\{\lambda_1(t), \ldots, \lambda_N(t)\}$. We require:

$$-\lambda_{\min}(t) \|\nabla E_O(\mathbf{s}(t))\|^2 \leq -\delta \|\nabla E_O(\mathbf{s}(t))\| \|\dot{\mathbf{s}}(t)\|\,,$$

or equivalently

$$\lambda_{\min}(t) \|\nabla E_O(\mathbf{s}(t))\| \geq \delta \|\dot{\mathbf{s}}(t)\|\,.$$

Note that $\|\dot{\mathbf{s}}(t)\| \leq \lambda_{\max}(t)) \|\nabla E_O(\mathbf{s}(t))\|$, where $\lambda_{\max}(t) = \max\{\lambda_1(t), \ldots, \lambda_N(t)\}$. Therefore:

$$\delta = \inf_{t > \tau} \frac{\lambda_{\min}(t)) \|\nabla E_O(\mathbf{s}(t))\|}{\|\dot{\mathbf{s}}(t)\|} \geq \inf_{t > \tau} \frac{\lambda_{\min}(t)}{\lambda_{\max}(t)} > 0.$$

We can then conclude that the p_i's will asymptotically converge to a unique critical configuration for E_O. $\square$

Remark 4.3 (Implementation by group of robots) To implement equation (6), it suffices that the robots exchange information about their positions (like for the inner-polygon approximation) and their local tangent.•

4.1 Discrete-time outer-polygon approximation algorithms

It is easy to prove that an algorithm analogous to Algorithm 1 in the previous section guarantees convergence to the critical configuration of E_O. We state the analogous results here omitting the corresponding proof. Given a strictly convex set Q, define $q_{\min}\colon (\partial Q)^2 \to \partial Q$ as follows: $q_{\min}(q_1, q_2)$ is the point of the counterclockwise arc from q_1 to q_2 whose tangent to ∂Q satisfies $d_i^- = d_i^+$. Note that $q_{\min}(q_1, q_2)$ minimizes $q \mapsto \mathrm{Area}(P_O(q_1, q, q_2))$.

Algorithm 3. At each discrete time instant $k \in \mathbb{N}$ and for each node $i \in \{1, \dots, N\}$ define:

$$p_i(k+1) = \begin{cases} q_{\min}(p_{i-1}(k), p_{i+1}(k)), & \text{if } i = k \mod N, \\ p_i(k), & \text{if } i \neq k \mod N. \end{cases} \tag{7}$$

Theorem 4.4 (Convergence of Algorithm 3) *If $k \mapsto \eta(k) = (p_1(k), \dots, p_N(k))$ denotes a trajectory of the dynamical system (7), then $E_O \circ \eta$ is monotonic non-increasing and η converges asymptotically to the set of critical configurations of E_O.*

Remark 4.5 Similarly to Algorithm 2 in the inner-polygon approximation problem, it is possible to design a discrete time algorithm based on admissible quintuplets. Such algorithm would have limitations similar to the ones of Algorithm 2 and we do not present it here in the interest of brevity. •

5 "Outer minus inner" polygon approximation algorithms

In this section we provide a novel expression for the partial derivative of the symmetric difference error E_S (under the assumption that the outer polygon is bounded) and we design a new gradient decent algorithm.

Lemma 5.1 (Partial derivative of E_S) *If (p_i, p_{i+1}) is cc-tangent-connected, then the area of the triangle formed by the segment $\overline{p_{i+1}p_i}$ and the rays $\ell^+(p_i)$ and $\ell^-(p_{i+1})$ is*

$$A_i(p_i, p_{i+1}, \mathbf{n}_i, \mathbf{n}_{i+1}) = \frac{1}{2}\frac{(\mathbf{n}_i \cdot (p_i - p_{i+1}))(\mathbf{n}_{i+1} \cdot (p_i - p_{i+1}))}{(\mathbf{n}_i \times \mathbf{n}_{i+1})_3},$$

where, for $\mathbf{n}_i = (n_i^1, n_i^2)$ and $\mathbf{n}_{i+1} = (n_{i+1}^1, n_{i+1}^2)$, we let $(\mathbf{n}_i \times \mathbf{n}_{i+1})_3 = n_i^1 n_{i+1}^2 - n_i^2 n_{i+1}^1$. Furthermore,

$$\frac{\partial E_S(p_1, \dots, \gamma(s_i), \dots, p_N)}{\partial s_i} = \left(\frac{\partial A_{i-1}}{\partial p_i} + \frac{\partial A_i}{\partial p_i} - \kappa(s_i)\left(\frac{\partial A_{i-1}}{\partial \mathbf{n}_i} + \frac{\partial A_i}{\partial \mathbf{n}_i}\right)\right) \cdot \mathbf{t}_i.$$

The proof of the first statement is based upon elementary calculations and is omitted in the interest of space; the second statement is an immediate consequence of equation (1). Explicit expressions for the relevant partial derivatives in Lemma 5.1 are given as follows. If we set $p_i = (x_i, y_i)$, $\mathbf{n}_i = (n_i^1, n_i^2)$ and $\mathbf{n}_{i-1} \times \mathbf{n}_i^+ := n_{i-1}^1 n_i^2 + n_i^1 n_{i-1}^2$, then

$$\begin{aligned} \frac{\partial A_{i-1}}{\partial x_i} &= \frac{(p_i - p_{i-1}) \cdot (\, 2n_{i-1}^1 n_i^1,\, \mathbf{n}_{i-1} \times \mathbf{n}_i^+ \,)}{2(\mathbf{n}_{i-1} \times \mathbf{n}_i^+)}, \\ \frac{\partial A_{i-1}}{\partial y_i} &= \frac{(p_i - p_{i-1}) \cdot (\, \mathbf{n}_{i-1} \times \mathbf{n}_i^+,\, 2n_{i-1}^1 n_i^1 \,)}{2(\mathbf{n}_{i-1} \times \mathbf{n}_i^+)}, \\ \frac{\partial A_{i-1}}{\partial n_i^1} &= \frac{n_i^2 (\mathbf{n}_{i-1} \cdot (p_i - p_{i-1})^2)}{2(\mathbf{n}_{i-1} \times \mathbf{n}_i^+)^2}, \\ \frac{\partial A_{i-1}}{\partial n_i^2} &= \frac{n_i^1 (\mathbf{n}_{i-1} \cdot (p_i - p_{i-1})^2)}{2(\mathbf{n}_{i-1} \times \mathbf{n}_i^+)}. \end{aligned}$$

We are now ready to state the properties of the gradient flow of E_S. We omit the proof of the following theorem as it closely parallels that of Theorem 3.1.

Theorem 5.2 (Gradient flow for E_S) *If $t \mapsto \eta(t) = (p_1(t), \dots, p_N(t))$ denotes a trajectory of the dynamical system*

$$\dot{p}_i = -\,\mathbf{t}_i \left(\frac{\partial A_{i-1}}{\partial p_i} + \frac{\partial A_i}{\partial p_i} - \kappa(s_i)\left(\frac{\partial A_{i-1}}{\partial \mathbf{n}_i} + \frac{\partial A_i}{\partial \mathbf{n}_i}\right)\right) \cdot \mathbf{t}_i\,, \tag{8}$$

with $E_S \circ \eta(0) < +\infty$, then $E_S \circ \eta$ is monotonic non-increasing and η converges asymptotically to the set of critical configurations of E_S. Furthermore, if the boundary ∂Q is analytic, then η converges asymptotically to a critical configuration.

Remark 5.3 (Implementation by group of robots) Even for this scenario, the robots can move along the gradient of E_S relying upon information that is available to them through one-hop communication and through sensing of local tangent and curvature data. •

6 Simulations

Figure 5 shows the implementation results of the three continuous time descent algorithms described

in equations (2), (6), and (8). The eleven nodes are on the contour described by $\gamma(\theta) = (2.1 + \sin(2\pi\theta))(\cos(2\pi\theta), \sin(2\pi\theta))^T$, for $\theta \in [0, 1)$. Figure 6

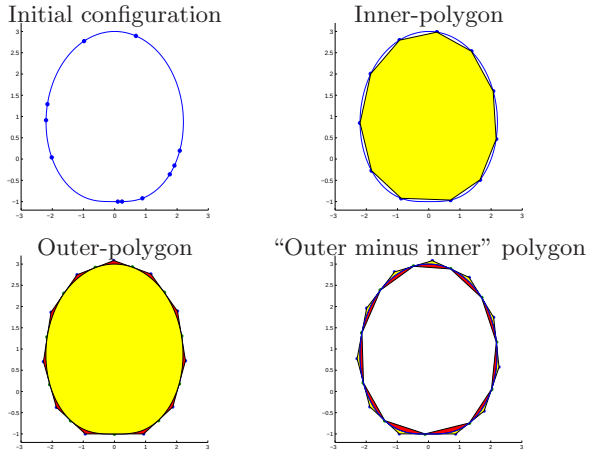

Fig. 5. From left to right and from top to bottom: initial condition of eleven nodes on a convex boundary, final condition after the implementation of the inner-polygon, outer-polygon, and "outer minus inner" polygon approximation algorithms.

shows the implementation results of the discrete-time Algorithm 2 described in (5).

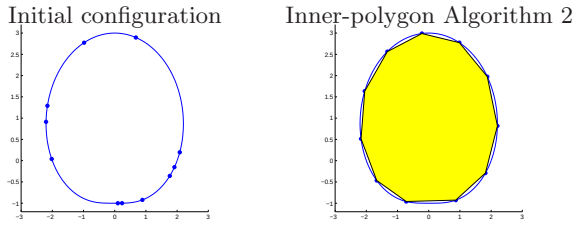

Fig. 6. From left to right: initial condition of eleven nodes on a convex boundary and final condition after the implementation of Algorithm 2. In this particular case the final point configuration satisfies the critical point condition of equation (3).

7 Conclusions

We have discussed various geometric optimization problems and corresponding gradient flows. Future works will focus on nonsmooth contours such as polygons, nonconvex sets, and more general algorithms for optimal interpolation of boundaries.

Acknowledgements

This material is based upon work supported by NSF Awards CMS-0442041, CMS-0643679 and ONR Award N00014-07-1-0721. An early version of this work appeared in the 2006 IEEE Conference in Decision and Control with title "Distributed algorithms for polygonal approximation of convex contours."

References

[1] P.-A. Absil, R. Mahony, and B. Andrews. Convergence of the iterates of descent methods for analytic cost functions. *SIAM Journal on Control and Optimization*, 6(2):531–547, 2005.

[2] D. W. Casbeer, D. B. Kingston, R. W. Beard, T. W. Mclain, S.-M. Li, and R. Mehra. Cooperative forest fire surveillance using a team of small unmanned air vehicles. *International Journal of Systems Sciences*, 37(6):351–360, 2006.

[3] J. Clark and R. Fierro. Mobile robotic sensors for perimeter detection and tracking. *ISA Transactions*, 46(1):3–13, 2007.

[4] M. P. Do Carmo. *Differential Geometry of Curves and Surfaces*. Prentice Hall, Englewood Cliffs, NJ, 1976.

[5] P. M. Gruber. Approximation of convex bodies. In P. M. Gruber and J. M. Willis, editors, *Convexity and its Applications*, pages 131–162. Birkhäuser Verlag, 1983.

[6] U. Helmke and J. B. Moore. *Optimization and Dynamical Systems*. Springer Verlag, New York, 1994.

[7] H. H. Johnson and A. Vogt. A geometric method for approximating convex arcs. *SIAM Journal on Applied Mathematics*, 38(2):317–325, 1980.

[8] M. Kass, A. Witkin, and D. Terzopoulos. Snakes: Active contour models. *International Journal of Computer Vision*, 1(4):321–331, 1987.

[9] C. Lageman. Konvergenz reell-analytischer gradientenähnlicher systeme. Master's thesis, Institut für Mathematik, Universität Würzburg, Germany, 2002.

[10] S. Łojasiewicz. Sur les trajectoires du gradient d'une fonction analytique. *Seminari di Geometria 1982-1983*, pages 115–117, 1984. Istituto di Geometria, Dipartimento di Matematica, Università di Bologna, Italy.

[11] D. Marthaler and A. L. Bertozzi. Tracking environmental level sets with autonomous vehicles. In S. Butenko, R. Murphey, and P. M. Pardalos, editors, *Recent Developments in Cooperative Control and Optimization*, pages 317–330. Kluwer Academic Publishers, 2003.

[12] L. Scardovi, A. Sarlette, and R. Sepulchre. Synchronization and balancing on the N-torus. *Systems & Control Letters*, 56(5):335–341, 2007.

[13] E. Trost. Über eine Extremalaufgabe. *Nieuw Archief voor Wiskunde*, 2:1–3, 1949.

[14] F. Zhang and N. E. Leonard. Generating contour plots using multiple sensor platforms. In *IEEE Swarm Intelligence Symposium*, pages 309–316, Pasadena, CA, June 2005.